Metabolic Engineering 88 (2025) 250–260

Contents lists available at ScienceDirect

Metabolic Engineering

journal homepage: www.elsevier.com/locate/meteng

Exploring and increased acetate biosynthesis in *Synechocystis* PCC 6803 through insertion of a heterologous phosphoketolase and overexpressing phosphotransacetylase

Stamatina Roussou [a], Minmin Pan [b], Jens O. Krömer [b], Peter Lindblad [a,*]

[a] Microbial Chemistry, Department of Chemistry-Ångström Laboratory, Uppsala University, Uppsala, Sweden
[b] Systems Biotechnology, Department of Microbial Biotechnology, Helmholtz Centre for Environmental Research – UFZ, 04318, Leipzig, Germany

ARTICLE INFO

Keywords:
Cyanobacteria
Phosphoketolase
Acetyl phosphate
G3P
FBP
Pyruvate
Acetyl-CoA
Acetate
Calvin-Benson-Bassham

ABSTRACT

Acetate is a biological anion with many applications in the chemical and food industries. In addition to being a common microbial fermentative end-product, acetate can be produced by photosynthetic cyanobacteria from CO_2 using solar energy. Using wild-type cells of the unicellular model cyanobacterium *Synechocystis* PCC 6803 only low levels of acetate are observed outside the cells. By inserting a heterologous phosphoketolase (PKPa) in the *acs* locus, encoding acetyl-CoA synthetase responsible for the irreversible conversion of acetate to acetyl-CoA, an increased level of 40 times was observed. Metabolite analyses indicate an enhanced Calvin-Benson-Bassham cycle, based on increased levels of glyceraldehyde 3-phosphate and fructose-1,6-biphosphate, while the decreased levels of 3-phosphoglycerate and pyruvate suggest a quick consumption of the fixed carbon. Acetyl-P and erythrose-4-phosphate showed significantly increased levels, as products of phosphoketolase, while acetyl-CoA remained stable through the experiment. The results of intra- and extra-cellular acetate levels clearly demonstrate an efficient excretion of produced acetate from the cells in the engineered strain. Knock-out of ach and pta showed a reduction in acetate production however, it was not as low as in cells with a single knock-out of ach. Overexpressing acetyl-CoA hydrolase (Ach) and acetate kinase (AckA) did not significantly increase production. In contrast, overexpressing phosphotransacetylase (Pta) in cells containing an inserted PKPa resulted in 80 times more acetate reaching 2.3 g/L after 14 days of cultivation.

1. Introduction

Acetate, an important carbon metabolite in cyanobacteria, can be considered a storage product and precursor for further metabolism and growth in microorganisms (Liu et al., 2019; Phue et al., 2010). Acetic acid, the conjugate acid of acetate, is an industrial bulk chemical for the generation of products for the chemical industry and used in the food industry. In particular, it serves as a presentative and is used as vinegar or as solvent for the production of polyethylene terephthalate (PET) (Pal and Nayak, 2017). More recently, acetate has been used as a source of carbon (Kiefer et al., 2021) with microorganisms able to catabolize acetate for the production of selected valuable chemicals. The main routes to commercially produce acetate are through petrochemical and biotechnological procedures. Additional technologies include lignocellulose depolymerization, microbial gas fermentation, microbial electrosynthesis, and anaerobic oxidation of methane (Kiefer et al., 2021).

A wide variety of microorganisms produce acetate from sugars as a side product of the metabolism, especially under anaerobic conditions (Pan et al., 2021; Ahmad et al., 2024, Işık et al., 2024). Photosynthetic microorganisms, including algae and cyanobacteria, convert carbon dioxide (CO_2) and solar energy into hydrocarbons to grow and form biomass. Acetate, a common metabolite, is often produced during cultivation in darkness under anaerobic conditions in green algae (*Chlamydomonas reinhardii*) (Yang et al., 2014) and cyanobacteria (Akiyama and Osanai, 2024). Only few studies have addressed the production of acetate during photosynthetic growth. For example, Zhou et al. (2012) studied acetate production in *Synechocystis* PCC 6803 (thereafter *Synechocystis*), a model unicellular cyanobacterium, under light conditions in combination with nitrogen and phosphate starvation, while the *phaEC* locus (encoding the synthesis of PHB) was knocked out, and reported 290 ± 12 mg/L after 4 days of cultivation. However, Du et al. (2018) were not able to quantify acetate under regular light growth

* Corresponding author.
E-mail address: peter.lindblad@kemi.uu.se (P. Lindblad).

https://doi.org/10.1016/j.ymben.2025.01.008
Received 18 October 2024; Received in revised form 14 January 2025; Accepted 21 January 2025
Available online 23 January 2025
1096-7176/© 2025 The Authors. Published by Elsevier Inc. on behalf of International Metabolic Engineering Society. This is an open access article under the CC BY license (http://creativecommons.org/licenses/by/4.0/).

conditions. The production of acetate can be a result of anabolic pathways under light limited conditions but none of them are directly connected to the carbon metabolism (Du et al., 2018). Other pathways of acetate production in *Synechocystis* are either through acetyl-phosphate (acetyl-P) or through acetyl-CoA, see Fig. 1. The acetyl-P to acetate reaction takes place through acetate kinase (AckA) which is a reversible reaction generating ATP (Atteia et al., 2013). On the other hand, acetyl-coenzyme A synthetase (Acs) performs the irreversible reaction of acetate catalysis to acetyl-CoA with the parallel hydrolysis of ATP to AMP, followed by acetyl-CoA hydrolase (Ach) which catalyse the formation of acetyl-CoA to acetate (Carpine et al., 2017). Lastly, another enzyme of the acetate pathway that is worth mentioning is phosphotransacetylase (Pta), which catalyses the reversible transformation of acetyl-P to acetyl-CoA. Acetate is secreted from the cells as the cell membranes are permeable to weak organic acids, most likely a passive process. Additionally, there is evidence for the presence of acetate exporters in eukaryotes such as *Candida glabrata* (Romão et al., 2017) and yeast (Piper et al., 2001). However, there is, to our knowledge, no evidence for the presence of an acetate transporter in *Synechocystis* or any other cyanobacteria strains.

Acetyl-CoA is a central metabolite from which a wide range of applications in diverse microorganisms are possible (Liu et al., 2019, Phue et al., 2010. There are several options to increase the carbon flux to acetyl-P and acetyl-CoA, with one of them being via a phosphoketolase (PK) (Liu et al., 2019; Xiong et al., 2016). The PK pathway in cyanobacteria was until recently uncharacterized (Lu et al., 2023) while it has been studied in bacteria like *Bifidobacteria* (Fandi et al., 2001) and *Lactobacillus* (Posthuma et al., 2002). In *Synechococcus elongatus* PCC 7942 the PK regulates carbon fixation, especially during light and dark transitions (Lu et al., 2023). The enzyme was discovered to be active in *Synechocystis* under heterotrophic and nitrogen starvation conditions, including darkness, while knocking out of the putative PK gene in *Synechocystis* led to decreased level of acetate under the same conditions (Lu et al., 2023). The role of the enzyme is to convert xylulose 5-phosphate (Xu5P, 5 carbons) or fructose 6-phosphate (F6P, 6 carbons) to acetyl-P (2 carbons) and glyceraldehyde 3-phosphate (3PGA, 3 carbons) or erythrose 4-phosphate (E4P, 4 carbons) (Xiong et al., 2016), see Fig. 1.

Heterologous PKs have been inserted in *Synechocystis* intending to increase the acetyl-CoA pool for 1-butanol production during nitrogen starvation (Anfelt et al., 2015) or under photosynthetic growth conditions (Liu et al., 2019) and as well as for PHB production (Carpine et al., 2017). The pathway acts as a carbon-conserving shunt compared to glycolysis where there is a loss of one carbon for each acetyl-CoA being derived from pyruvate (Bogorad et al., 2013).

In this study, we express a codon-optimized PK from *Pseudomonas aeruginosa* (thereafter PKPa) (Liu et al., 2019), with the aim of increasing the production of acetate under photosynthetic growth conditions. The strain was also used for metabolomic studies to analyse the influence of its expression on the CBB cycle and other major metabolites. Moreover, knock outs and overexpressions were done in *Synechocystis* to examine the native acetate pathways. We knocked out genes encoding Pta and Ach or Pta and AckA as well as only AckA or Ach, to address competing pathways, respectively.

The genes encoding the native AckA and Ach, and a codon optimized Pta originally from *Bacillus subtilis* were overexpressed individually using a self replicator vector. The latter resulted in maximal acetate production under photosynthetic growth conditions.

2. Materials and methods

2.1. Cultivation conditions of Escherichia coli and Synechocystis sp. strain PCC 6803

Escherichia coli (*E. coli*) strains were grown under 37 °C with LB medium either in liquid or on plates made with the addition of 1.5 % agar (w/v). *Synechocystis* sp. strain PCC 6803 (*Synechocystis*) strains

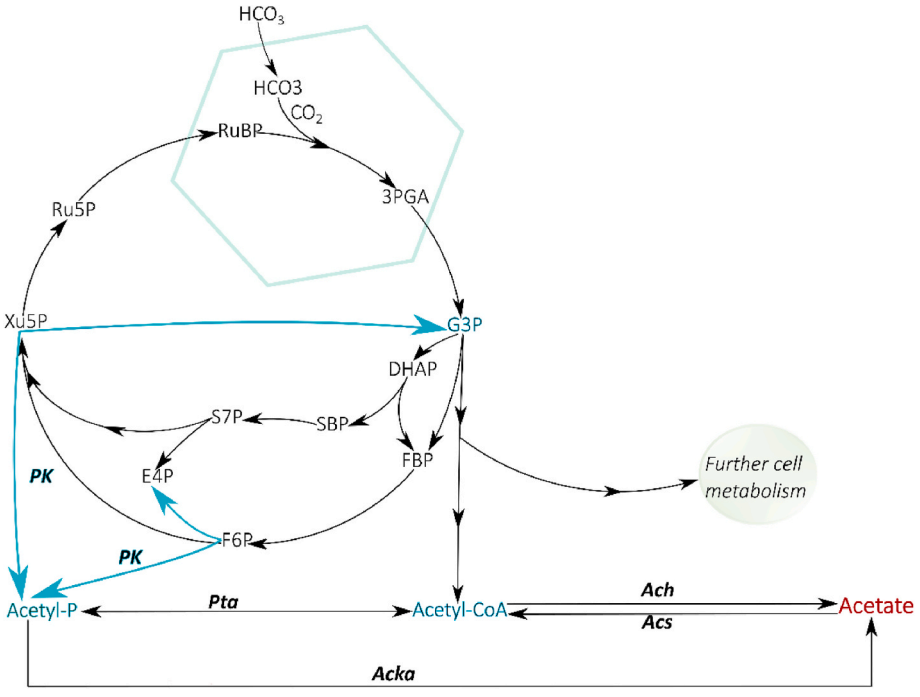

Fig. 1. Outline of the Calvin-Benson-Basshmam (CBB) cycle, carboxysome and the native acetate production pathway. The carboxysome is representing by the green hexagonal, the CBB cycle is represented by solid black lines while the inserted phosphoketolase is represented with solid blue lines.The intermediates are represented using abbreviations; 3PGA, 3-phosphoglycerate; G3P, glyceraldehyde-3-phosphate; DHAP, dihydroxyacetone phosphate; FBP, fructose-1,6-bisphosphate; SBP, sedoheptulose-1,7-bisphosphate; F6P, fructose-6-phosphate; S7P, sedoheptulose-7-phosphate; E4P, erythrose-4-phosphate; Xu5P, xylulose-5-phosphate; R5P, ribose-5-phosphate; Ru5P, ribulose-5-phosphate; RuBP, ribulose-1,5-bisphosphate. Enzymes; pta, phosphotransacetylase; acka, acetate kinase; acs, acetyl-CoA synthetase; ach; acetyl-CoA hydrolase and PK; phosphoketolase. With blue colour are highlighted the main substrates for acetate biosynthesis and with red the acetate is highlighted. (For interpretation of the references to colour in this figure legend, the reader is referred to the Web version of this article.)

were cultivated under 30 °C and 65 μmol photons $m^{-2}s^{-1}$. The medium used was BG11 (Stanier et al., 1971), both in liquid cultures and 1.5 % agar (w/v) plates. Three different antibiotics (Sigma-Aldrich) were used in both organisms; kanamycin, spectinomycin, and erythromycin. For the first two, a final concentration of 50 μg/ml was used for both microorganisms while for erythromycin 200 μg/ml was used for *E. coli* and 50 μg/ml for *Synechocystis.* In the case of more than one antibiotic, half of the concentrations were used.

2.2. Plasmid construction and transformation to Synechocystis

The plasmids used in this study are presented in Tables S2 and S3. Plasmids used to develop the knock outs strains were based on the previously reported pEERM vectors (Englund et al., 2015). They can be named suicide plasmids as they are not able to replicate in the cyanobacteria cell. Homologous recombination was performed using 1000 bp homologous arms upstream and downstream of the gene of interest, respectively. The sequences to be used were amplified from *Synechocystis* genome and before joined with the desired gene of interest and the antibiotic cassette through overlap extension PCR. The final product was ligated with the backbone vector through linear ligation. The backbone vector and the final product were phosphorylated in either the 5′ or the 3' DNA end and ligated together. The ligation product was transformed to competent *E. coli* T7 cells (NEB) followed by colony PCR and sequencing in order to verify correct clone.

When verified, natural transformation was used to engineer the cyanobacterium genome (Table S1). The *Synechocystis* strains were cultivated to OD_{750} = 0.5–1.2 in liquid BG11 with the appropriate antibiotics. Then the cells were collected through centrifugation (5000×*g* for 10 min), washed twice with fresh BG11 medium, and resuspended at OD_{750} = 2.5 in 400 μl of BG11. The next step was to mix the cells with the suicide plasmid in a final concentration of 10 μg/μl before the mixture was incubated at low light at 30 °C for 4–5 h. Thereafter the cells were spread on membrane filters on BG11 plates without antibiotics and the following day the membrane was transferred to BG11 plates with the selection antibiotic(s). After 7–10 days isolated colonies were regrown in fresh plates and colony PCR was performed. Positive clones were incubated in 6 well TC plates (Sarstedt) with the appropriate antibiotic(s) and propagated until complete integration of the desired cassette in the genome. The segregation was checked with PCR using specific primers.

The plasmids used for overexpression (Table S3) are self-replicated plasmids based on the pSHDY vector (Behle and Axmann, 2022). Two of the genes that were overexpressed (*ach* and *ack*A) were amplified from the genome while to overexpress the *pta* gene a smaller codon optimized version of the gene was used (Liu et al., 2019). The expression cassette, including the promoter, the terminator, and the spectinomycin cassette, was constructed with overlap expression PCR and ligated to the backbone vector as above and the same verification process was followed.

The self-replicated plasmids were inserted into the *Synechocystis* cells through three parental conjugation, as described previously (Roussou et al., 2021). Generated engineered strains were verified through colony PCRs with corresponding primers.

All amplifications and overlap extension PCRs were performed with corresponding primers (Supplementary material, Table S4) using polymerase Phusion DNA Polymerase (Thermo Fisher Scientific). The colony PCRs were performed with DreamTaq DNA polymerase Polymerase (Thermo Fisher Scientific). Heterogenous genes used were codon optimized and synthesize by GenScript.

2.3. Protein analysis

Synechocystis cell cultures were grown up to OD_{750} = 2 and pelleted through centrifugation followed by resuspension with 2 ml of phosphate-buffered saline pH 7.5 (PBS buffer). The step was repeated and the final volume was 200 μl of PBS with the addition of 3 μl of protease inhibitors and the samples were kept on ice. Acid-washed glass beads (425–600 mm diameter, Sigma-Aldrich) were added to each sample, and the cells were disrupted through a bead homogenizer, Precellys-24 Beadbeater (Bertin Instruments). The program includes 3 000×*g* for 4 times, 30 s each, with 2 min of rest on ice between each spin. After a final short centrifugation at 13 000×*g* (4 °C), the supernatant was transferred to a new tube. The protein concentration was estimated through the DC protein assay (Bio-Rad). An SDS-PAGE, Mini-PROTEAN TGXt gels (Bio-Rad), was used in order to analyse 10 μg of each crude protein sample. Then the gel proteins were transferred to a "Trans-Blot Turbo Transfer Pack'' membrane (Bio-Rad) and the corresponding tagged proteins were detected by using anti-Strep-taq antibodies (abcam) followed by anti-Rabbit tag (Biorad) secondary antibody through the standard immunoblotting technique. The identified proteins were visualized by incubation with HRP substrate before imaging with the program Quality One.

2.4. Acetate production experiments and quantifications

Pre-cultures of the production experiment were cultivated in 6-well TC plates until the mid-log phase. The starting OD_{750} was calculated to be 0.2 and all experimental cultures were in triplicates and were cultivated in 100 mL Erlenmeyer flasks (VWR) with a total volume of 20 ml BG11 containing 50 mM $NaHCO_3$ (Sigma-Aldrich) and the corresponding antibiotics under 65 μmol photons $m^{-2}s^{-1}$ and 30 °C. The $NaHCO_3$ was used as a supplement to the inorganic carbon source that leads to higher levels of acetate production. Every two days the cultures were sampled and 2 ml were removed for analysis while 2 ml of fresh BG11 medium supplemented with 500 mM $NaHCO_3$ to keep the volume constant. The same day, the pH of the culture was measured and adjusted with the use of 37% HCl (Sigma-Aldrich) to a pH between 7 and 8. The optical density was measured every 2 days using 200 μl of diluted sample in 96-well plates and a micro-plate reader (HIDEX, Plate Chameleon). Chlorophyll *a* was extracted from the 2 ml that were sampled from the cell cultures. The samples were centrifuged for 7 min at maximum speed, the supernatant was used for acetate quantification and the pellet was re-suspended in 1 ml cold methanol (+4 °C) before it was homogenized by vortex and incubated for 1 h in +4 °C. After a second centrifugation, the absorbances were measured at A_{470} A_{665}, and A_{720}. The final chlorophyll *a* concentration and carotenoids were calculated by the equations by Ritchie (2006) and Wellburn (1994), respectively.

To quantify the acetate concentration, the supernatant of the 2 ml was filtered with a 0.22 μm filter. Then 0.5 ml of the filtrated supernatant was mixed with 10 μl 50 μM potassium hydrogen phthalate ($HOOCC_6H_4COOK$), serving as an internal standard, and 90 μl of deuterium oxide (both from Sigma-Aldrich). The total volume of 0.6 ml was transferred to an NMR tube and analysed by NMR. A JEOL (400 YH magnet) Resonance 400 MHz spectrometer was used and the obtained ^1H NMR spectra were analysed by Mestrenova software.

2.5. Metabolites extraction and analysis

In order to analyse metabolite extraction, the experiment was based on the setup described in paragraph 2.4. However, modifications were performed to serve the exact purpose of this experiment. Three biological replicates were sampled every day of the experiment that lasted 4 days. This indicates the existence of 4 sets of 3 biological replicates. Every day, 20 ml of culture were used for analysis reasons, 2 ml for OD and acetate production measurements, and 18 ml for metabolite extraction.

These 18 ml of cultures were filtered (Whatman CN filters, 0.2 μm) and then washed twice with isotonic NaCl solution at the experimental temperature and directly after the membrane containing the filtered cells was snap freeze at liquid nitrogen. The whole process was

completed in less than 1 min.

For the metabolite extraction, a biphasic-ice cold solvent mixture of methanol, chloroform, and water was used, 1 ml of methanol-chloroform and 2.5 ml of H_2O. The water contained the following internal standards; 20 μmol/l azelaic acid, 15 μmol/l D-norvaline, and 25 μmol/l ribitol (Sigma-Aldrich). The mixture of cells and solvents went through ice-cold ultrasonication and bead vortex. Then ice-cold water was added up to 12 ml, the samples were lyophilized before dissolved in 2 ml H_2O. Samples of 750 μl were lyophilized again in clear glass gas chromatography (GC) vials (VWR). The GC samples were analysed quantified with an Orbitrap system (OrbitrapExploris 240 Mass Spectrometer, ThermoFisher) coupled with either an ion-chromatograph (ICS-6000, organic acid column, Dionex IonPac^{TM}CS19-4 μm, RFIC, 2 × 250 mm) or an HPLC system (HC-C18(2) column, 4.6 × 150 mm, 5 μm, 400 bar, Agilent). All organic acids and sugar phosphates were quantified with IC-MS, while acetyl-CoA was quantified with HPLC-MS. Specifically, for the running of the IC-MS, the flow rate of the makeup pump, the regenerant pump, and the main pump (ICS-6000) was 0.15 ml/min (methanol), 0.5 ml/min (Milli-Q water), and 0.38 ml/min, respectively. The column and compartment temperature were set to 30 and 20 °C, respectively. EGC 500 KOH was employed to generate the flow gradient as described in Table S6. The detection of acetyl-CoA was done with HPLC-MS, 10 mM ammonium formate (pH 3) either in milliQ water (eluent A) or in 90% acetonitrile (eluent B) were employed with the flow gradient described in Table S7. The column temperature was 25 °C and a UV detector with 220 nm was applied. The MS scan range was set as 40–900 with a detection resolution of 15000. For both IC/HPLC-MS systems, the H-ESI ion source was applied with a static spray voltage mode of 3500 V (positive ion) and 2500 V (negative ion). Temperatures were set to 325 °C for the Ion transferable and 300 °C for the vaporizer. A full scan method with dd MS^2 detection (secondary MS) was applied. Softwares Chromeleon Console (version 7) and Compound Discoverer 3.3 were used for the data analyses.

3. Results

3.1. The insertion of PKPa is responsible for increased extracellular acetate levels

Several strains were constructed to examine the effect of heterologous expression of *PKPa* on the acetate production in *Synechocystis*. An integration vector was constructed containing the *PKPa* gene under the control of the strong constitutive promoter P*trcRiboJ*, and a kanamycin resistance cassette. The integration vector was targeting the *acs* locus (*sll0542*) since this gene encodes acetyl-CoA synthetase, an enzyme responsible for the irreversible conversion of acetate to acetyl-CoA (Fig. 1). Furthermore, an integration vector was designed to knock out the *acs* locus with the parallel insertion of the kanamycin resistance cassette to identify any effect on the acetate production independent of the *PKPa* insertion. These two integration vectors were transformed to WT *Synechocystis* and generated strains WT_Δacs and WT_PKPa_Δacs, respectively. Lastly, WT_ΔNSI a *Synechocystis* strain engineered with the kanamycin cassette on NSI (*slr0168*) served as a control to investigate if there is any effect of the antibiotic existence on the acetate production levels (Rodrigues et al., 2023). As shown in Fig. 2a, the growth of the cells did not show any significant differences, even though it is noticeable that the WT and WT_ΔNSI grew slightly better than the other two. In Fig. 2b and c the extracellular acetate production per volume and per cell (normalized per OD) are shown, respectively. Acetate production is low and very similar between the WT and WT_ΔNSI indicating that the expression of the antibiotic does not influence the acetate production levels. Higher levels are noticeable both in strains WT_Δacs and WT_PKPa_Δacs. However, the first showed 4 times increase while the strain expressing the *PKPa* showed 40 times increase, both per volume and when normalized per OD, compared to WT *Synechocystis* cells. These results clearly demonstrate that the insertion of *PKPa* has a much stronger effect on the acetate production that the knock-out of the *acs* gene, and its insertion is necessary for the higher acetate levels observed.

An alternative approach to investigate acetate production has also been studied through the insertion of pyruvate oxidase (PoxB). Two versions of the enzymes were selected, one from *E. coli* and one from *K. pneumoniae*, and codon optimized for *Synechocystis* (Table S5). The promoter chosen for these studies was the P*trc*BCD which was integrated in the *ddh* site of the chromosome (slr1556) encoding D-lactate dehydrogenase which is producing lactate from the precursor pyruvate. As seen in Fig. S1 the production of acetate did not increase while the PoxB was expressed in the cells (Fig. S2).

3.2. Insertion of PKPa significantly increases the 3PGA and the acetyl-P pool sizes

The significant increase in extracellular acetate level, depending on the expression of phosphoketolase led to the next experimental design where we studied the differences in the levels of main metabolites. For this scope the strains WT_PKPa_Δacs and WT_ΔNSI were selected, the second one served as control. The strains were cultivated for 4 days, the growth and acetate production levels are shown in Figure S3. The growth experiment was performed as already discussed in section 2.5. Some of the metabolites show clear changes either up or down regulated when the fold change was studied. 3PGA and fructose-1,6-biphosphate (FBP) showed increased levels throughout the experiment while the next metabolite of the CBB cycle, 3-phosphoglycerate (G3P), is below the control levels. For the last one, the actual amount of it did not exceed 229 μmol/OD/L on the last day of the experiment, with a maximum amount quantified being 442.8 μmol/OD/L on Day 2 while the control strain showed greater fluctuation with values between 358 and 1195.6 μmol/OD/L. 3PGA has also been quantified, WT_PKPa_Δacs values ranged between 201.6 and 487.5 μmol/OD/L, a significant increase compared to the control which was quantified between 77.4 and 107.3 μmol/OD/L (Figure S4). Moving on in the study of metabolites in the CBB cycle, an important increase of E4P is noticeable, the highest increase compared to the rest metabolites (Fig. 3). Increased levels of sedoheptulose-7-phosphate (S7P), Xu5P, and ribulose-5-phosphate (Ru5P) are noticeable in the first 2 days of the experiment while both of them are less than in the control the following days. More specifically, for the Ru5P the range of the control strain was identified between 285.4 and 435.1 μmol/OD/L while for the strain overexpressing the phosphoketolase it was between 276.4 and 378.4 μmol/OD/L, both with a maximum of 636 μmol/OD on days 3 and 2, respectively (Figure S4). Lower than the control is also observed for fructose-6-phosphate throughout the experimental period.

Down-stream the CBB cycle, acetyl-P, pyruvate, acetyl-CoA. and intracellular acetate were quantified. The acetyl-P showed a significant increase throughout the experiment with values reaching 2.6 mmol/OD/L compared to 1.6 mmol/OD/L in the control strain, while pyruvate showed decreased levels, the control strain fluctuated between 107.1 and 182 mmol/OD/L, much higher than the 60–73 mmol/OD/L observed on the WT_PKPa_Δacs strain (Fig. 3 and S.4). Decreased levels were also observed for the intracellular acetate levels while acetyl-CoA was at similar levels as the control strain, with an exception on Day 2. Specifically, the intracellular acetate of the WT_ΔNSI was measured between 18.3 and 13.4 μmol/OD/L compared to 1.2–7.2 μmol/OD/L in the WT_PKPa_Δacs strain. The acetyl-CoA levels in both strains was measured between 9.4 and 11.1 μmol/OD/L.

3.3. Knocking out genes of the acetate pathway affects differently on the acetate production levels

In the next step of this study, the effect of knocking out different genes of the acetate pathway was investigated using the strain WT_PKPa_Δacs as the background/control strain. Four different strains were generated for this scope, and at least two rounds of transformations

a.

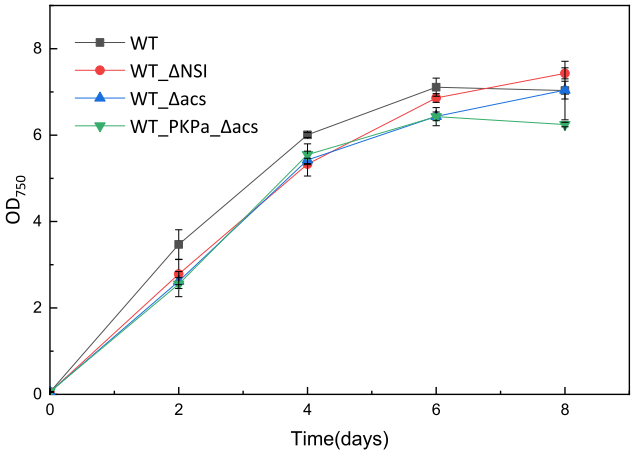

b.

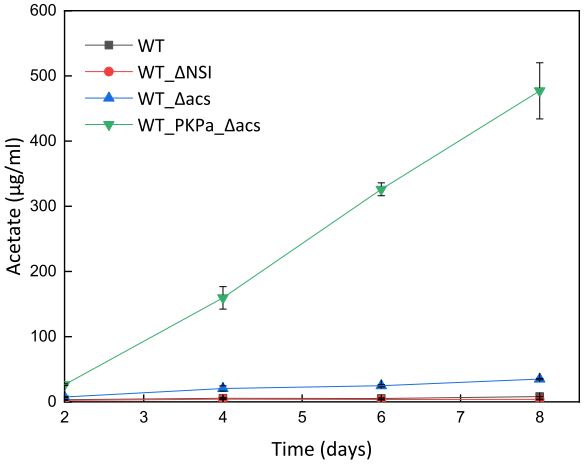

c.

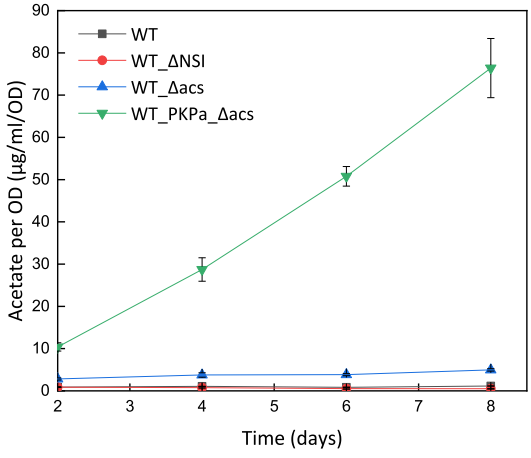

(caption on next column)

Fig. 2. Growth and acetate production in WT *Synechocystis* PCC 6803 as well as engineered strains with the kanamycin resistance cassette in the NSI or *acs* locus, and in the strain engineered to contain the gene encoding PKP*a* in the *acs* locus. Shown are the growth of the cells (a), the acetate production per volume (b) and per cell (c). The strains were cultivated under 65 μmol photons $m^{-2}s^{-1}$. Every second day 2 ml were sampled from the cell cultures and replaced with fresh BG11 containing $NaHCO_3$ (final concentration 50 mM). At the same pH was adjusted with HCl (7–8). Acetate production and OD were measured on days 2, 4, 6 and 8. The results are represented as mean ± SD of the three biological replicates.

and full segregations were performed. In order to study the efficiency of Ach, under the insertion of the *PKPa*, a strain with double knock out of *ackA* and *pta* genes was developed (WT_PKPa_Δacs_Δacka_Δpta), and a strain with antibiotic resistance to three different antibiotics; Km, Em, and Sm. Knocking out both *pta* and *ach* make it possible to address the AckA efficiency. Since these two genes are located close to each other in the genome, both of them were knocked out using a single integration vector (IVE Δach_pta, EmR). In order to be able to be comparable with the strain WT_PKPa_Δacs_Δacka_Δpta, a second transformation was made in the NSI loci to insert antibiotic resistance to spectinomycin generating the strain WT_PKPa_Δacs_Δach _Δpta_ΔNSI. Two additional strains were constructed to investigate the efficiency of *pta* combined either with the *acka* (WT_PKPa_Δacs_Δach_ΔNSI) or with *ach* (WT_PKPa_Δacs_Δacka_ΔNSI) both containing the SmR cassette in the NSI. Fig. 4a shows the growth, measured as OD, of the strains during 14 days when the OD of the control strain (WT_PKPa_Δacs) started to decrease. No major differences among the strains in growth were observed. The chlorophyll *a* and carotenoids levels followed the same trend (Figure S5). The highest chlorophyll *a* concentration was observed on Day 6 while the lowest was on Day 14. In Fig. 4b and c the extracellular acetate production per volume and normalized per OD are shown, respectively. In all 4 strains, it is noticeable that the acetate production is lower than the control strain. In more detail, the strains WT_PKPa_Δacs_Δach _Δpta_ΔNSI and WT_PKPa_Δacs_Δacka_ΔNSI showed similar levels, all of them reached only half of the production of the control strain. This indicates that the *acka* and the *pta* + *ach* pathway reached independently similar acetate production levels when *PKPa* is present in the cells. The other two strains showed a major drop in acetate production as the strain WT_PKPa_Δacs_Δach_ΔNSI produced 0.15 times less than the control while WT_PKPa_Δacs_Δacka_Δpta reached 0.2 times the production of the strain WT_PKPa_Δacs. These results indicated that the *ach* gene is responsible for a similar production level as the *pta* + *acka* pathway. The same trends are observed when the acetate production is normalized to the chlorophyll *a* concentration (Figure S6).

3.4. Overexpression of pta leads to a significant increase in acetate production

In order to study the effect of overexpressing different genes of the acetate pathway, self-replication vectors were constructed and transformed through conjugation to strain WT_PKPa_Δacs. The native genes *ach* and *acka* were chosen as well as a codon-optimized version of Bs*Pta* (Lui et al., 2019). Two different promoter sequences were tested, P*psbA2* and P*trc*RiboJ. The first one is a strong native light regulated promoter (Englund et al., 2016) while the second is a strong heterologous constitutive promoter (Huang et al., 2010) combined with a self-cleaving ribozyme (Lou et al., 2012) to enhance both transcription and translation. The growth of the cells, as shown in Fig. 5a, was similar between the strains, and similar results were observed for the carotenoid concentrations while the chlorophyll *a* level diverted slightly (Fig. S7). More specifically, strains WT_PKPa_Δacs + Ptrc_BsPta and WT_PKPa_Δacs + PsbA2_ach showed 10% less chlorophyll *a* concentration while strains WT_PKPa_Δacs + Ptrc_ach and WT_PKPa_Δacs + PsbA2_acka approximately 20% less chlorophyll *a*. The two strains WT_PKPa_Δacs + PsbA2_BsPta and WT_PKPa_Δacs + Ptrc_acka showed almost the same

a.

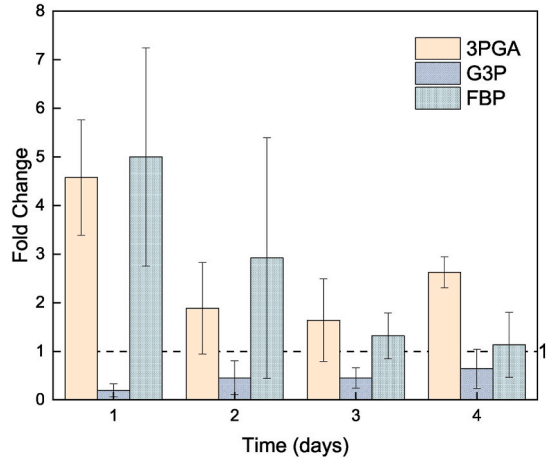

b.

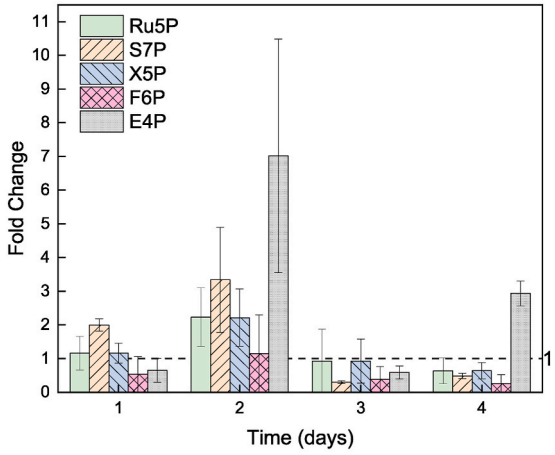

c.

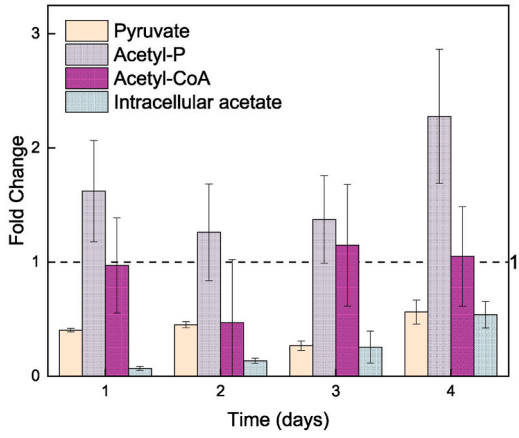

(caption on next column)

Fig. 3. Fold Changes of the main metabolites analysed between the strains WT_PKPa_Δacs and WT_ΔNSI. The second strain served as the control and it is representing as the dotted line horizontally with the number 1 and based on these values the fold change of the experimental strain was calculated. The metabolites analysed included the carbon fixation part of the CBB cycle followed by the reduction part of 3PGA to G3P and production of FBP (a). An analysis was also performed in the regeneration part of the cycle (b) and finally on the products leaving the CBB in connection with the acetate production (c). Remarkable results are the increase of 3PGA followed by a decrease on G3P, the overall increased levels of the regeneration part of the cycle as well as the increase of acetyl-P combined with the relatively stable levels of acetyl-CoA. Finally, a significant result is the decreased level of intracellular acetate compared to the increase of the extracellular.

levels as the control strain (WT_PKPa_Δacs). Fig. 5b and c shows the extracellular acetate production per volume and when normalized per OD while Figure S8 shows the acetate production normalized per chlorophyll *a*. The strains overexpressing *pta* showed the highest production levels of acetate, approximately twice of the control for the strain overexpressing *pta* under the P*psbA2* promoter (WT_PKPa_Δacs + PsbA2_BsPta) and almost 3 times more for the strain where the *pta* was under the control of P*trc*RiboJ (WT_PKPa_Δacs + Ptrc_BsPta). Even though this is the average increase, the strain WT_PKPa_Δacs + PsbA2_BsPta showed higher production than the WT_PKPa_Δacs + Ptrc_BsPta in the last 2 sampling points (days 12 and 14) while it showed the highest acetate titter in the last day of the experiment, 2.3 g/L. However, the strains overexpressing the *ach* gene did not show significantly increased acetate titers. Under the control of P*psbA2*, the titter was 20% higher than the control (WT_PKPa_Δacs + PsbA2_ach) while under the strong constitutive promoter (WT_PKPa_Δacs + Ptrc_ach) it was even lower than in the control strain reaching only 0.9 times its production. Similar results were observed for the strains overexpressing the *ack*A gene, specifically the strain WT_PKPa_Δacs + PsbA2_acka produced almost the same as the control strain while the strain WT_PKPa_Δacs + Ptrc_acka produced around 10% less acetate than WT_PKPa_Δacs. These results indicated that Pta is a key enzyme in acetate production.

4. Discussion

This present study focused on exploring acetate production in *Synechocystis* and achieved significantly higher production yield, 2.3 g/L. Acetate is mainly produced via acetyl-P and acetyl-CoA, metabolites which we aimed to enhance through insertion of a phosphoketolase and overexpression of the key pathway enzymes.

PKs are enzymes related to glycolysis that use X5P or F6P for the production of acetyl-P and G3P or E4P, respectively (Moriyama et al., 2015). Except acetyl-P the other compounds are primarily part of the Calvin-Benson Bassham (CBB) cycle, the main carbon fixation pathway in cyanobacteria (Liang et al., 2018b). Originally, the enzyme is active during heterotrophic conditions in cyanobacteria (Xiong et al., 2016) and it is important in ATP production combined with the acetate kinase (Lu et al., 2023). Heterologous PKs have been introduced in *Synechocystis* PCC 6803 to increase the pool of acetyl-CoA for the production of chemicals and fuels (Liu et al., 2019). We investigated the effect of the expression of a codon-optimized version of a phosphoketolase from *Pseudomonas aeruginosa* (PKPa). PKPa was previously selected as the optimal PK, out of the nine examined, for 1-butanol production in *Synechocystis* (Liu et al., 2019).

The expression of PKPa was under a strong constitutive promoter, P*trc*RiboJ, the latter part encoding a self-cleaving ribozyme to potentially improve the protein translation (Liu et al., 2019; Lou et al., 2012). The cultivation conditions were optimized for acetate production and the pH adjusted every second day (Miao et al., 2018). At the same time points, $NaHCO_3$ was added to the cultures. These two steps were found to be crucial for the growth of the cells as at this pH range, the carbon

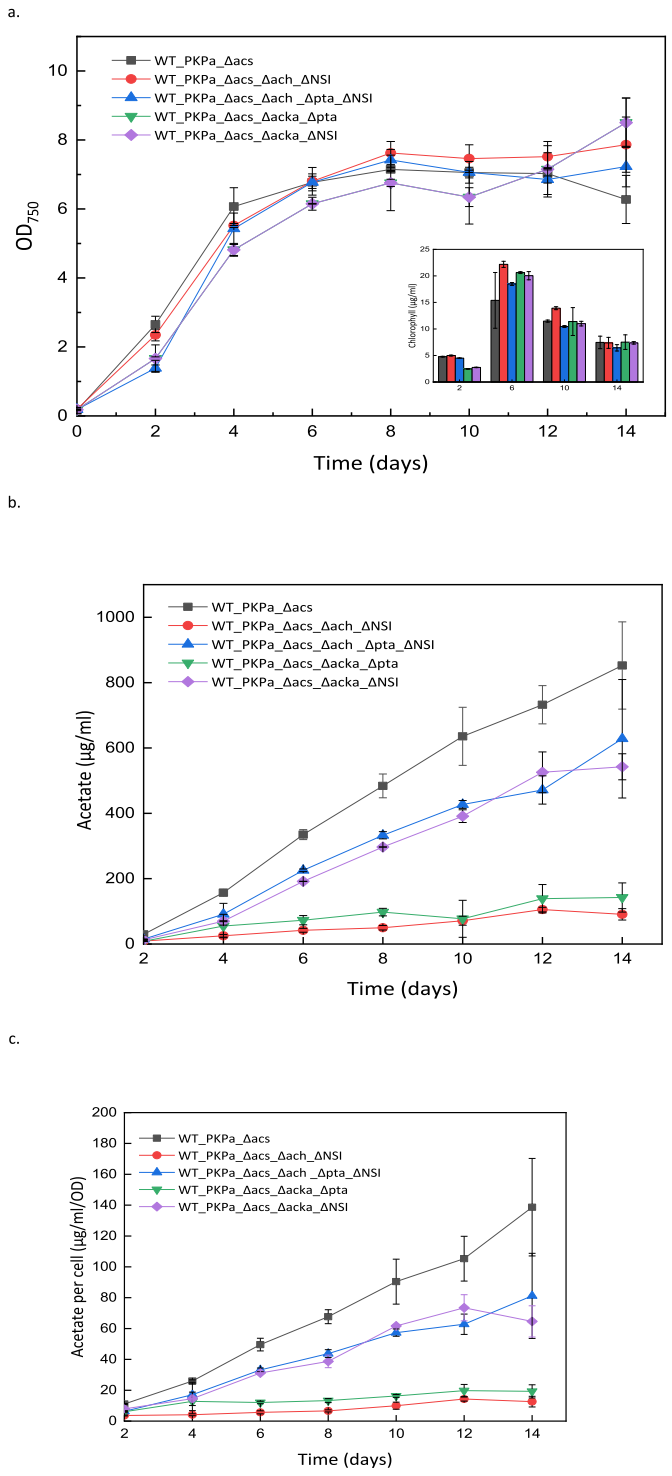

Fig. 4. Growth, representing by OD and chlorophyll concentration, and acetate production in strains engineered to express PKPa (WT_PKPa_Δacs) with knockout to one (WT_PKPa_Δacs_Δach_ΔNSI and WT_PKPa_Δacs_Δacka_ΔNSI) or two (WT_PKPa_Δacs_Δach _Δpta_ΔNSI and WT_PKPa_Δacs_Δacka_Δpta) enzymes of the acetate pathway. Shown are the growth of the cells and chlorophyll *a* concentration (a), the acetate production per volume (b) and per cell/OD (c). The strains were cultivated under 65 μmol photons m-2s-1. Every second day 2 ml were sampled from the cell cultures and were replaced with fresh BG11 containing NaHCO3, final concentration 50 mM. At the same day the pH was adjusted with HCl to 7–8. Acetate production and OD were measured on days 2, 4, 6, 8, 10, 12 and 14 while characteristic days of the chlorophyll *a* are presented for days 2, 6, 10 and 14. The results are represented as mean ± SD of the three biological replicates.

remains in the HCO_3^- form which can be diffused into the carboxysome. Then, the carbonic anhydrases release the CO_2 which is then fixed by RubisCO (Durall et al., 2020).

Furthermore, the ratio between the acetic acid and the acetate ($CH3COOH/CH3COO^-$) is pH dependent (Proietti Tocca et al., 2024). In microalgae, concentrations between 0.68 and 3.45 mM (41–207 mg/L) of acetic acid have shown to inhibit growth, the reason is acidification of the cytosol (Proietti Tocca et al., 2024). The exact concentration is strain dependent. The threshold for *Synechocystis* is not known but addition of external acetate up to 30 mM (corresponding to 1.6 g/L) does not influence growth or the pH of the culture (Thiel et al., 2017). However, acetic acid is a weak acid with a pKa of 4.75 meaning that at higher pH than the pKa, the ratio of acetic acid is rapidly dropping. We observed a maximal acetate production of 2.3 g/L, higher than 1.6 g/L, without any reduced growth. Additionally, the acetate was rapidly exported from the cells. The toxicity of acetate to the organism has not been further studied (Proietti Tocca et al., 2024).

In order to analyse the effects of PKPa on the acetate production compared to the unmodified strain, we constructed several control strains. First, the presence of an antibiotic did not affect the production of acetate, wild type and modified cells with antibiotic resistance showed similar acetate production with a maximum of 8 μg acetate/ml. Unfortunately, there are no reports on acetate production in wild-type *Synechocystis* under phototrophic conditions as the acetate pathway is mostly studied during darkness and heterotrophic growth conditions (Xiong et al., 2016). The PKPa expression cassette was inserted in the acetyl-coenzyme A synthetase (*acs*) site. Acs is responsible for catalysis of acetate to acetyl-CoA and it is known as the main pathway for acetate assimilation (Du et al., 2018). A knock-out strain showed 4 times more acetate production. So, from this experiment, it is clear that the insertion and expression of the PKPa in the *acs* site is responsible for the significantly increased, 40 times, acetate production.

The specific phosphoketolase expressed has a higher affinity to X5P than to F6P (Petrareanu et al., 2014) which would lead to higher yield of G3P compared to E4P and an increased yield of acetyl-P. In order to analyse the effect of the insertion of PKPa on the *acs* site we performed metabolite analyses on the strain WT_PKPa_Δacs with WT_ΔNSI serving as the control strain. It is noticeable that the intracellular acetate levels do not follow at all the trend of extracellular acetate levels experimentally determined outside the cells. The acetate production in this 4 days experiment kept the same trend as the previous experiment, meaning the acetate produced from WT_PKPa_Δacs was much higher than from the control strain. However, the intracellular acetate, especially in days 1 and 2 in the WT_PKPa_Δacs is significantly lower than in the control strain. This result leads to the conclusion that the cells overproducing acetate also export it faster. Accumulation of acetate in the cytoplasm has been shown to affect the growth rate in the green algae *C. reinhardtii* (Proietti Tocca et al., 2024), similar mechanism(s) may be present in *Synechocystis* leading to an increased export of acetate. The mechanism of acetate export from the cells is not known, the main theory is a passive diffusion out of the cells. To the best of our knowledge, no acetate exporter has been identified in *Synechocystis* but this result indicates a possible trans-membrane transporter to avoid the creation of stress in the cytoplasmic environment.

Phosphoketolase is an enzyme that channels more carbon from the CBB cycle so the analysis of metabolites was focused on the changes of its components. One clear result is the increased level of 3-phosphoglycerate (3PGA), the outcome of RubisCO's activity. 3PGA is constantly higher in the strain expressing the phosphoketolase compared to the control strain. This may lead to the conclusion that there is a higher carbon fixation in the engineered overproducing acetate strain. An earlier study (Liang et al., 2018a) stated that the introduction of a carbon sink can lead to increased biomass accumulation, indicating a higher carbon fixation, and subsequent, further turnover, in the cells. The stably increased values of 3PGA clearly support this statement as it seems that the CBB cycle works at higher rates in the strain that has a

a.

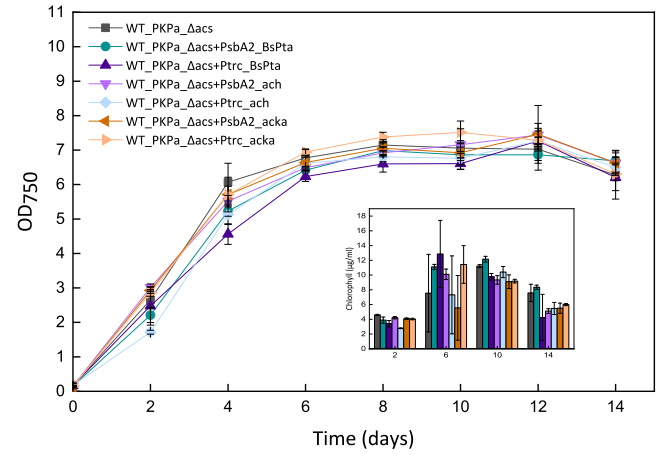

b.

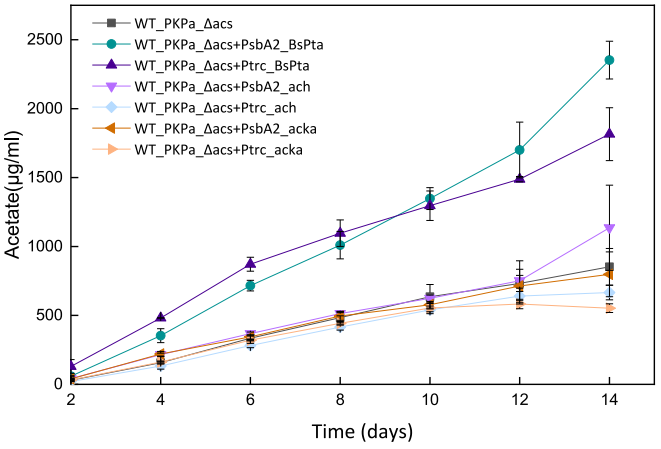

c.

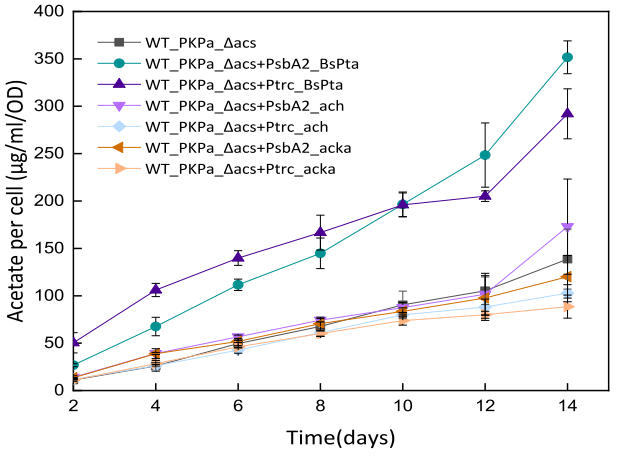

(caption on next column)

Fig. 5. Growth, representing by OD and chlorophyll concentration, and acetate productionin strains engineered to express PKPa (and WT_PKPa_Δacs) and one of the enzymes of the acetate production pathway (Bs*Pta*, *ach* and *acka*) under either P*psbA2* or P*trcRiboJ* promoter. Shown are the growth of the cells and chlorophyll *a* concentration (a), the acetate production per volume (b) and per cell (c). The strains were cultivated under 65 μmol photons $m^{-2}s^{-1}$ while every two days 2 ml were sampled from the cell cultures and were replaced with fresh BG11 with $NaHCO_3$ with final concentration 50 mM. At the same day the pH was adjusted with HCl (7–8). Acetate production and OD were measured on days 2,4,6,8, 10,12 and 14 while characteristic days of the chlorophyll are presented (days 2,6,10 and 14). The results are represented as mean ± SD of the three biological replicates.

carbon sink while the growth rate of the cells did not significantly change. The next step of the CBB cycle is the reduction stage where the 3PGA converts to glyceraldehyde-3-phosphate (G3P) with a parallel consumption of ATP and NADPH. Despite the noticeable increase in 3PGA, this pattern is not followed in the levels of G3P. One possible explanation for this result is a quick consumption of G3P to other metabolic pathways, beyond the CBB cycle. This may be the reason why the levels of fructose-1,6-bisphosphate (FBP), a metabolite that is part of the next stage of the CBB cycle, the RuBP regeneration stage, follows mainly the pattern of 3PGA than its precursor.

At the regeneration stage, we observe differences in the levels of central metabolites, as the phosphoketolase channels carbon from specifically Xu5P or/and F6P. Both of these molecules showed increased levels in the WT_PKPa_Δacs strain, at least for the first days of the experiment. A drop is noticeable after the third day, a pattern similar to sedoheptulose-7 phosphate (S7P) and also to the ribulose-5-phosphate (RuBP). The increased fold change of these metabolites combined with the increased levels of 3PGA and the decreased fold change of G3P, shows that overall the CBB cycle works faster and the reduction stage is critical for the rate of carbon fixation and subsequent carbon accumulation. There is also a significant increase in the E4P, significantly higher than the other 3 metabolites of the regeneration part, X5P, F6P, and S7P. A theory that may justify this result, is that the E4P is also a product of PK the increase observed is a combined result of the overall improvement of the carbon fixation. The positive effect on the CBB cycle can be concluded from the overall increase of the main metabolites of the cycle, except the G3P, which is the main compound exiting the cycle and quickly consumed from the cell metabolism.

The metabolites chosen to be analysed down-stream of the CBB cycle are pyruvate, acetyl-CoA, and acetyl-P, all in their relationship to the observed increased level of acetate outside the cells. The pyruvate follows the pattern of G3P, a reasonable result as this central metabolite derives from this molecule. The acetyl-CoA levels seem to remain at similar levels while the acetyl-P is clearly higher in WT_PKPa_Δacs. Despite the drop of pyruvate, the levels of acetyl-CoA remain stable. This may indicate that the increased level of acetyl-P influenced the acetyl-CoA through the phosphotransacetylase (Pta). Another conclusion that may be formulated is that the stability of the acetyl-CoA is of high importance for the cell metabolism, and in order to remain unchanged the increased level of acetyl-P is metabolised to acetate, a side product for the cell.

Acetyl-P is a central metabolite in many organisms with an active role in post translational modifications, e.g. in *E. coli* (Kuhn et al., 2014) also as a regulator (McCleary and Stock, 1994), and proven to have a significant role in lysine acetylation in *E. coli* (Weinert et al., 2013) and *Streptomyces* (Takahashi-Íñiguez and Flores, 2023). In *Synechocystis* a role in signalling has been identified (Morrison et al., 2005). More precisely it is involved in the DspA-dependent signalling important for the degradation of chlorophyll-protein complexes.

Acetate kinase (AckA) and phosphotransacetylase (Pta) are two key enzymes controlling the intracellular pool of acetyl-P, and the reactions they catalyse are acetyl-P + ADP ↔ acetate + ATP and acetyl-CoA + Pi ↔ acetyl-P + CoA, respectively. When it comes to acetate production,

acetyl-P is a key compound. It can either be used as a substrate for AckA, or through acetyl-CoA by the Pta-Ach route. It is clear that the acetate levels are controlled by several pathways and the expression of PKPa results in a significant increase in the synthesis of acetate. Strains with disruptions in the different pathways for acetate synthesis were developed. WT_PKPa_Δacs_ Δach_ ΔNSI was designed to study the effect of knocking-out Ach which is catalysing the reaction from acetyl-CoA to acetate. In this strain, the production was based on ackA while Pta was still active. In the following strain, WT_PKPa_Δacs_ Δach_pta_ ΔNSI, the production of acetate is mainly based on the expression of AckA while the *pta* is also knocked out. The aim of the construction of the strain WT_PKPa_Δacs_ Δacka_ Δpta is to investigate acetate production when only Ach is active, it is the mirror strain of the WT_PKPa_Δacs_ Δach_ ΔNSI while finally, the strain WT_PKPa_Δacs_ Δacka_ ΔNSI investigated the route Pta and Ach while AckA is knocked out.

Both when normalized per OD and per chlorophyll *a*, acetate production followed the growth of the cells, a result that has been indicated in the literature (Du et al., 2018). Since acetate is a side product of the metabolism it makes sense that when the production is lower the cells grow better. We could also argue that the AckA influences less the acetate production compared to the other strains. Since there are no extended studies on the role of acetyl-P as a global regulator and signal molecule in *Synechocystis,* we cannot know exactly how the disruption of AckA may influence the metabolism and regulation of the cell while the gene is known as the main acetate production route under dark and anaerobic conditions (Akiyama and Osanai, 2024). One possibility is that the presence of Pta may drag surplus of acetyl-P to the production of acetyl-CoA and following metabolic routes of the cell, in the competition for substrate between Pta and AckA, the preference is Pta. The following strain tested, WT_PKPa_Δacs_Δach_pta_ΔNSI supported this hypothesis since the cells produced significantly more acetate compared to the previous knocked out strain. One possible explanation is that since the Pta is not active, surplus acetyl-P was channelled to acetate via AckA. The next two strains focused on the effect of Ach on acetate production, with and without the expression of *pta*. The route Pta-Ach showed the highest production, through the knock-out strains, indicating that the increased pool of acetyl-P is being converted into acetyl-CoA which leads to production of acetate through Ach. Worth mentioning is the fact that, unlike other organisms like *E. coli* (Dittrich et al., 2005), the *pta* gene is not in an operon with the *ack*A gene but with the *ach*. It has also been reported that deleting *ach* can increase the synthesis of products derived from acetyl-CoA such as 1-butanol (Liu et al., 2019). Furthermore, the Pta-AckA route controls the acetate fluxes in *E. coli* (Enjalbert et al., 2017), a pattern that is not followed in *Synechocystis* according to our experimental results. When the *pta* gene is knocked out, meaning the strain WT_PKPa_Δacs_ Δacka_ Δpta, there is only very low production of acetate. It has been shown that disruption of the *pta* resulted in lower acetate production in *Synechocystis* under dark anaerobic conditions as well as with limitations on nitrogen and phosphorus (Zhou et al., 2012), we encountered similar results but under phototrophic conditions.

In the next step, the effects of over expressing different genes of the acetate pathway in combination with strong expression of PKPa were studied. The *ach* and *acka* genes were amplified from *Synechocystis*'s genome while for the *pta* we used a smaller and codon-optimized version derived from *Bacillus subtilis* (Liu et al., 2019), *BsPta*. The aim was to investigate if an extra copy of the respective gene(s), will affect the production of acetate.

Both strains overexpressing *pta* showed high level of production, at least 2 times more acetate than the control strain (WT_PKPa_Δacs), especially the strain with PtrcRiboJ as promoter (3 times increased production when normalized to chlorophyll *a* concentration). The maximal level of acetate was observed on day 14 by strain WT_PKPa_PsbA2_Bspta reaching 2.352 mg acetate/ml (2.3 g/L). Acetate production in heterotrophs such as *E. coli* can be higher (Zhu et al., 2024) but, to our knowledge, this is the highest production observed in photosynthetic microorganisms under any photoautotrophic growth condition. It is worth mentioning that this strain showed slower growth compared to the rest, supporting the conclusion made earlier, that since the acetate is a side product, higher production of it may indicate less channelling of carbon to biomass, resulting in slower growth rate. The overexpression of *ach* and *ack*A did not show any improvement in the production. However, in both cases, it was observed that when the genes were under the control of P*sbA2* promoter the production was slightly higher than in the control while under the strong constitutive promoter P*trc*RiboJ the production was even less than in the strain WT_PKPa_Δacs. This is a clear indicator that a strong expression does not always reach the desirable results as it is highly possible that the accumulation of these enzymes can create stress for the cells. A clear comparison between Ach and AckA is not possible with this data set, even though the acetate level in strain WT_PKPa_PsbA2_ach was slightly higher than the strain overexpressing *acka* under the same promoter. Most of the strains contained on average a lower level of chlorophyll *a* and carotenoids during the experimental period. It has been demonstrated that external addition of acetate in the media, as in mixotrophic growth conditions, in *Chlamydomonas reinhardtii* can cause reduction in photosynthetic activity including lower chlorophyll pigment contents (Liu et al., 2009) and down-regulation of RubisCO (Proietti Tocca et al., 2024). Similar effects have also been reported for *Synechocystis* and there are theories that acetate competes with bicarbonate/carbonate on PSII which may lead to a reduction of O_2 evolution (Thiel et al., 2017). In the same study, it also discussed that the addition of acetate in the media resulted in an increased production of carotenoids, as a protective mechanism against a stressful condition. It cannot be taken for granted that the cells followed the same strategy as the organism can respond differently when a compound is added externally in the culture or when it is produced in the cells so further investigations are needed.

Since the production increased in strains overexpression of *pta* combined with the results from the knockout experimental strains, we can conclude that the phosphoketolase and phosphotransacetylase enzymes are crucial for the improvement of acetate production. The combined expression of these enzymes increased the acetyl-CoA pool, demonstrated in yeast (Hellgren et al., 2020) and it was also proven by Song et al. (2021), especially with the disruption of *ack*A in *Synechocystis*. However, it was not shown that acetyl-CoA is favoured compared to acetyl-P for acetate production, especially under photosynthetic growth conditions in *Synechocystis*. It is known that insertion of *pta* from *E. coli* in *Synechococcus* PCC 7942 increased the acetate production via acetyl-CoA. In this case the acetyl-CoA pool was increased through the overexpression of the Pyruvate Dehydrogenase Complex (PDH) (Hirokawa et al., 2020).

Even though the overexpression of either *ach* or *ackA* did not reveal a clear preference of pathway for the acetate production, the increased levels observed under *pta* overexpression with an increased pool of acetyl-P can drive to the conclusion that the PKPa-BsPta leads to significantly increased acetate synthesis compared to PKPa-AckA. These results are interesting since it has been reported that phosphoketolase leads to acetyl-P accumulation and in a non-yeast fungus it is channelled to acetate through AckA (Wolfe et al., 2005). In addition, this reaction produces ATP so AckA may also act as a regulator for ATP production in the cells.

Finally, an alternative idea to increase the flow of carbon would be to use pyruvate as a building molecule. In *E. coli* and other organisms such as *Klebsiella pneumoniae*, pyruvate oxidase, a peripheral membrane protein, (PoxB) is a key enzyme for the production of acetate from pyruvate, especially in the stationary growth phase (Dittrich et al., 2005; Lin et al., 2016). This enzyme leads to increased acetate, CO_2, and ubiquinol production using pyruvate, ubiquinone, and H_2O. PoxB was introduced in *Synechocystis* under the control of the PtrcBCD promoter. However, there was no enhanced acetate production. One reason may be that the poxB was detected in the cytoplasm (Fig. S2). Another issue may be that poxB uses ubiquinone but *Synechocystis* produces plastoquinone with related structure and function (Dähnhardt et al., 2002).

5. Conclusions

Insertion of a heterologous phosphoketolase (PKPa) in the cyanobacterium *Synechocystis* PCC 6803 leads to increased levels of extracellular acetate, 40 times more than in wild-type (WT) cells. A metabolomic analysis revealed a complicated map of up and down regulations of key metabolites in the cell. The levels of 3PGA and FBP increased compared to in the WT strain while G3P decreased. These data indicate a faster CBB cycle and a higher carbon turnover. We also noticed a reduced level of pyruvate. In contrast, acetyl-P, a main product of the enzyme, increased, a pattern also noticed for the E4P, another product of the phosphoketolase. Despite the increase of the acetyl-P, we observed stable levels of acetyl-CoA, indicating an unaffected metabolite. An unexpected result of the metabolomic analysis, is the high difference observed between the intra-versus extra-cellular acetate levels between the strains examined, implying that the excretion of the acetate is maybe not only a passive diffusion mechanism.

To analyze the role of the two acetate production pathways, a series of knock out and overexpression experiments took place. The results show that Pta is a key enzyme of the process, while a clear comparison between Ach and AckA is not possible, even though there are strong indications that Ach affects the acetate production more compared to AckA. Interestingly, the genes encoding Pta and Ach are located in the same operon in *Synechocystis,* while it is generally more common that *pta* is in the same operon as the gene encoding Acka.

Overexpression of *pta* in combination with the insertion of PKPa led to a doubled acetate production reaching 2.3 g/L after 14 days of cultivation.

CRediT authorship contribution statement

Stamatina Roussou: Writing – review & editing, Writing – original draft, Visualization, Validation, Methodology, Investigation, Formal analysis, Data curation, Conceptualization. **Minmin Pan:** Writing – review & editing, Writing – original draft, Visualization, Validation, Methodology, Investigation, Formal analysis, Data curation. **Jens O. Krömer:** Writing – review & editing, Visualization, Supervision, Resources, Investigation, Funding acquisition. **Peter Lindblad:** Writing – review & editing, Visualization, Supervision, Resources, Investigation, Funding acquisition, Conceptualization.

Funding

This work was funded by the European Union's Horizon 2020 research and innovation programme under the grant agreement No. 101000733 (project PROMICON).

Acknowledgments

We would like to thank Dr Anna Arkhypchuk (Department of Chemistry-Ångström, Uppsala University) for all the help provided regarding the NMR analyses.

Appendix. ASupplementary data

Supplementary data to this article can be found online at https://doi.org/10.1016/j.ymben.2025.01.008.

Data availability

Data will be made available on request.

References

Ahmad, M., Ahmed, Z., Riaz, M., Yang, X., 2024. Modeling the linkage between climate-tech, energy transition, and CO2 emissions: do environmental regulations matter? Gondwana Res. 127, 131–143. https://doi.org/10.1016/j.gr.2023.04.003.

Akiyama, M., Osanai, T., 2024. Regulation of organic acid and hydrogen production by NADH/NAD+ ratio in *Synechocystis* sp. PCC 6803. Front. Microbiol. 14, 1332449. https://doi.org/10.3389/fmicb.2023.1332449.

Anfelt, J., Kaczmarzyk, D., Shabestary, K., Renberg, B., Rockberg, J., Nielsen, J., Uhlén, M., Hudson, E.P., 2015. Genetic and nutrient modulation of acetyl-CoA levels in *Synechocystis* for n-butanol production. Microb. Cell Fact. 14 (1), 167. https://doi.org/10.1186/s12934-015-0355-9.

Atteia, A., van Lis, R., Tielens, A.G.M., Martin, W.F., 2013. Anaerobic energy metabolism in unicellular photosynthetic eukaryotes. Biochim. Biophys. Acta (BBA) - Bioenergetics 1827 (2), 210–223. https://doi.org/10.1016/j.bbabio.2012.08.002.

Behle, A., Axmann, I.M., 2022. pSHDY: a new tool for genetic engineering of cyanobacteria. In: Zurbriggen, M.D. (Ed.), Plant Synthetic Biology: Methods and Protocols, Methods in Molecular Biology. Springer US, New York, NY, pp. 67–79. https://doi.org/10.1007/978-1-0716-1791-5_4.

Bogorad, I.W., Lin, T.-S., Liao, J.C., 2013. Synthetic non-oxidative glycolysis enables complete carbon conservation. Nature 502 (7473), 693–697. https://doi.org/10.1038/nature12575.

Carpine, R., Du, W., Olivieri, G., Pollio, A., Hellingwerf, K.J., Marzocchella, A., Branco dos Santos, F., 2017. Genetic engineering of *Synechocystis* sp. PCC 6803 for poly-β-hydroxybutyrate overproduction. Algal Res. 25, 117–127. https://doi.org/10.1016/j.algal.2017.05.013.

Dähnhardt, D., Falk, J., Appel, J., van der Kooij, T.A.W., Schulz-Friedrich, R., Krupinska, K., 2002. The hydroxyphenylpyruvate dioxygenase from *Synechocystis* sp. PCC 6803 is not required for plastoquinone biosynthesis. FEBS Lett. 523 (1–3), 177–181. https://doi.org/10.1016/S0014-5793(02)02978-2.

Dittrich, C.R., Bennett, G.N., San, K.-Y., 2005. Characterization of the acetate-producing pathways in *Escherichia coli*. Biotechnol. Prog. 21 (4), 1062–1067. https://doi.org/10.1021/bp050073s.

Du, W., Jongbloets, J.A., van Boxtel, C., Pineda Hernández, H., Lips, D., Oliver, B.G., Hellingwerf, K.J., Branco dos Santos, F., 2018. Alignment of microbial fitness with engineered product formation: obligatory coupling between acetate production and photoautotrophic growth. Biotechnol. Biofuels 11 (1), 38. https://doi.org/10.1186/s13068-018-1037-8.

Durall, C., Lindberg, P., Yu, J., Lindblad, P., 2020. Increased ethylene production by overexpressing phosphoenolpyruvate carboxylase in the cyanobacterium *Synechocystis* PCC 6803. Biotechnol. Biofuels 13 (1), 16. https://doi.org/10.1186/s13068-020-1653-y.

Englund, E., Andersen-Ranberg, J., Miao, R., Hamberger, B., Lindberg, P., 2015. Metabolic engineering of *Synechocystis* sp. PCC 6803 for production of the plant diterpenoid manoyl oxide. ACS Synth. Biol. 4 (12), 1270–1278. https://doi.org/10.1021/acssynbio.5b00070.

Englund, E., Liang, F., Lindberg, P., 2016. Evaluation of promoters and ribosome binding sites for biotechnological applications in the unicellular cyanobacterium *Synechocystis* sp. PCC 6803. Sci. Rep. 6 (1), 36640. https://doi.org/10.1038/srep36640.

Enjalbert, B., Millard, P., Dinclaux, M., Portais, J.-C., Létisse, F., 2017. Acetate fluxes in *Escherichia coli* are determined by the thermodynamic control of the pta-AckA pathway. Sci. Rep. 7 (1), 42135. https://doi.org/10.1038/srep42135.

Fandi, K.G., Ghazali, H.M., Yazid, A.M., Raha, A.R., 2001. Purification and N-terminal amino acid sequence of fructose-6-phosphate phosphoketolase from *bifidobacterium longum* BB536. Lett. Appl. Microbiol. 32 (4), 235–239. https://doi.org/10.1046/j.1472-765X.2001.00895.x.

Hellgren, J., Godina, A., Nielsen, J., Siewers, V., 2020. Promiscuous phosphoketolase and metabolic rewiring enables novel non-oxidative glycolysis in yeast for high-yield production of acetyl-CoA derived products. Metabol. Eng. 62, 150–160. https://doi.org/10.1016/j.ymben.2020.09.003.

Hirokawa, Y., Kubo, T., Soma, Y., Saruta, F., Hanai, T., 2020. Enhancement of acetyl-CoA flux for photosynthetic chemical production by pyruvate dehydrogenase Complex overexpression in *Synechococcus elongatus* PCC 7942. Metabol. Eng. 57, 23–30. https://doi.org/10.1016/j.ymben.2019.07.012.

Huang, H.-H., Camsund, D., Lindblad, P., Heidorn, T., 2010. Design and characterization of molecular tools for a Synthetic Biology approach towards developing cyanobacterial biotechnology. Nucleic Acids Res. 38 (8), 2577–2593. https://doi.org/10.1093/nar/gkq164.

Işık, C., Ongan, S., Ozdemir, D., Jabeen, G., Sharif, A., Alvarado, R., Amin, A., Rehman, A., 2024. Renewable energy, climate policy uncertainty, industrial production, domestic exports/Re-exports, and CO_2 emissions in the USA: a SVAR approach. Gondwana Res. 127, 156–164. https://doi.org/10.1016/j.gr.2023.08.019.

Kiefer, D., Merkel, M., Lilge, L., Henkel, M., Hausmann, R., 2021. From acetate to Bio-based products: underexploited potential for industrial biotechnology. Trends Biotechn. 39 (4), 397–411. https://doi.org/10.1016/j.tibtech.2020.09.004.

Kuhn, M.L., Zemaitaitis, B., Hu, L.I., Sahu, A., Sorensen, D., Minasov, G., Lima, B.P., Scholle, M., Mrksich, M., Anderson, W.F., Gibson, B.W., Schilling, B., Wolfe, A.J., 2014. Structural, kinetic and proteomic characterization of acetyl phosphate-dependent bacterial protein acetylation. PLoS One 9 (4), e94816. https://doi.org/10.1371/journal.pone.0094816.

Liang, F., Lindberg, P., Lindblad, P., 2018a. Engineering photoautotrophic carbon fixation for enhanced growth and productivity. Sustain. Energy Fuels 2 (12), 2583–2600. https://doi.org/10.1039/C8SE00281A.

Liang, F., Englund, E., Lindberg, P., Lindblad, P., 2018b. Engineered cyanobacteria with enhanced growth show increased ethanol production and higher biofuel to biomass ratio. Metabol. Eng. 46, 51–59. https://doi.org/10.1016/j.ymben.2018.02.006.

Lin, J., Zhang, Y., Xu, D., Xiang, G., Jia, Z., Fu, S., Gong, H., 2016. Deletion of poxB, pta, and ackA improves 1,3-propanediol production by *Klebsiella pneumoniae*. Appl. Microbiol. Biotechnol. 100 (6), 2775–2784. https://doi.org/10.1007/s00253-015-7237-2.

Liu, X., Duan, S., Li, A., Xu, N., Cai, Z., Hu, Z., 2009. Effects of organic carbon sources on growth, photosynthesis, and respiration of *Phaeodactylum tricornutum*. J. Appl. Phycol. 21 (2), 239–246. https://doi.org/10.1007/s10811-008-9355-z.

Liu, X., Miao, R., Lindberg, P., Lindblad, P., 2019. Modular engineering for efficient photosynthetic biosynthesis of 1-butanol from CO_2 in cyanobacteria. Energy Environ. Sci. 12 (9), 2765–2777. https://doi.org/10.1039/C9EE01214A.

Lou, C., Stanton, B., Chen, Y.-J., Munsky, B., Voigt, C.A., 2012. Ribozyme-based insulator parts buffer synthetic circuits from genetic context. Nat. Biotechnol. 30 (11), 1137–1142. https://doi.org/10.1038/nbt.2401.

Lu, K.-J., Chang, C.-W., Wang, C.-H., Chen, F.Y.-H., Huang, I.Y., Huang, P.-H., Yang, C.-H., Wu, H.-Y., Wu, W.-J., Hsu, K.-C., Ho, M.-C., Tsai, M.-D., Liao, J.C., 2023. An ATP-sensitive phosphoketolase regulates carbon fixation in cyanobacteria. Nat. Metab. 5 (7), 1111–1126. https://doi.org/10.1038/s42255-023-00831-w.

McCleary, W.R., Stock, J.B., 1994. Acetyl phosphate and the activation of two-component response regulators. J. Biol. Chem. 269 (50), 31567–31572. https://doi.org/10.1016/S0021-9258(18)31731-9.

Miao, R., Xie, H., Lindblad, P., 2018. Enhancement of photosynthetic isobutanol production in engineered cells of *Synechocystis* PCC 6803. Biotechn. Biofuels 11 (1). https://doi.org/10.1186/s13068-018-1268-8.

Moriyama, T., Tajima, N., Sekine, K., Sato, N., 2015. Characterization of three putative xylulose 5-phosphate/fructose 6-phosphate phosphoketolases in the cyanobacterium *anabaena* sp. PCC 7120. Biosci. Biotechn. Biochem. 79 (5), 767–774. https://doi.org/10.1080/09168451.2014.993357.

Morrison, S.S., Mullineaux, C.W., Ashby, M.K., 2005. The influence of acetyl phosphate on DspA signalling in the cyanobacterium *Synechocystis* sp. PCC 6803. BMC Microbiol. 5 (1), 47. https://doi.org/10.1186/14761-2180-5-47.

Pal, P., Nayak, J., 2017. Acetic acid production and purification: critical review towards process intensification. Sep. & Purific. Rev. 46 (1), 44–61. https://doi.org/10.1080/15422119.2016.1185017.

Pan, X., Zhao, L., Li, C., Angelidaki, I., Lv, N., Ning, J., Cai, G., Zhu, G., 2021. Deep insights into the network of acetate metabolism in anaerobic digestion: focusing on syntrophic acetate oxidation and homoacetogenesis. Water Res. 190, 116774. https://doi.org/10.1016/j.watres.2020.116774.

Petrareanu, G., Balasu, M.C., Vacaru, A.M., Munteanu, C.V.A., Ionescu, A.E., Matei, I., Szedlacsek, S.E., 2014. Phosphoketolases from *Lactococcus lactis, Leuconostoc mesenteroides* and *Pseudomonas aeruginosa*: dissimilar sequences, similar substrates but distinct enzymatic characteristics. Appl. Microbiol. Biotechnol. 98 (18), 7855–7867. https://doi.org/10.1007/s00253-014-5723-6.

Phue, J.-N., Lee, S.J., Kaufman, J.B., Negrete, A., Shiloach, J., 2010. Acetate accumulation through alternative metabolic pathways in ackA-pta-poxB-Triple mutant in *E. coli* B (BL21). Biotechnol. Lett. 32 (12), 1897–1903. https://doi.org/10.1007/s10529-010-0369-7.

Piper, P., Calderon, C.O., Hatzixanthis, K., Mollapour, M., 2001. Weak acid adaptation: the stress response that confers yeasts with resistance to organic acid food preservatives. Microbiol. 147 (10), 2635–2642. https://doi.org/10.1099/00221287-147-10-2635.

Posthuma, C.C., Bader, R., Engelmann, R., Postma, P.W., Hengstenberg, W., Pouwels, P. H., 2002. Expression of the xylulose 5-phosphate phosphoketolase gene, xpkA, from *Lactobacillus pentosus* MD363 is induced by sugars that are fermented via the phosphoketolase pathway and is repressed by glucose mediated by CcpA and the mannose phosphoenolpyruvate phosphotransferase system. Appl. Environ. Microbiol. 68 (2), 831–837. https://doi.org/10.1128/AEM.68.2.831-837.2002.

Proietti Tocca, G., Agostino, V., Menin, B., Tommasi, T., Fino, D., Di Caprio, F., 2024. Mixotrophic and heterotrophic growth of microalgae using acetate from different production processes. Rev. Environ. Sci. Biotechnol. 23, 93–132. https://doi.org/10.1007/s11157-024-09682-7.

Ritchie, R.J., 2006. Consistent sets of spectrophotometric chlorophyll equations for acetone, methanol and ethanol solvents. Photosynth. Res. 89 (1), 27–41. https://doi.org/10.1007/s11120-006-9065-9.

Rodrigues, J.S., Kovács, L., Lukeš, M., Höper, R., Steuer, R., Červený, J., Lindberg, P., Zavřel, T., 2023. Characterizing isoprene production in cyanobacteria – insights into the effects of light, temperature, and isoprene on *Synechocystis* sp. PCC 6803. Biores. Techn. 380, 129068. https://doi.org/10.1016/j.biortech.2023.129068.

Romão, D., Cavalheiro, M., Mil-Homens, D., Santos, R., Pais, P., Costa, C., Takahashi-Nakaguchi, A., Fialho, A.M., Chibana, H., Teixeira, M.C., 2017. A new determinant of *Candida glabrata* virulence: the acetate exporter CgDtr1. Front. Cell. Infect. Microbiol. 7, 00473. https://doi.org/10.3389/fcimb.2017.00473.

Roussou, S., Albergati, A., Liang, F., Lindblad, P., 2021. Engineered cyanobacteria with additional overexpression of selected calvin-benson-bassham enzymes show further increased ethanol production. Metabol. Eng. Commun. 12, e00161. https://doi.org/10.1016/j.mec.2021.e00161.

Song, X., Diao, J., Yao, J., Cui, J., Sun, T., Chen, L., Zhang, W., 2021. Engineering a central carbon metabolism pathway to increase the intracellular acetyl-CoA pool in *Synechocystis* sp. PCC 6803 grown under photomixotrophic conditions. ACS Synth. Biol. 10 (4), 836–846. https://doi.org/10.1021/acssynbio.0c00629.

Stanier, R.Y., Kunisawa, R., Mandel, M., Cohen-Bazire, G., 1971. Purification and properties of unicellular blue-green algae (order chroococcales). Bacteriol. Rev.s 35 (2), 171–205. https://doi.org/10.1128/mmbr.35.2.171-205.1971.

Takahashi-Íñiguez, T., Flores, M.E., 2023. Acetyl phosphate acetylates proteins of *Streptomyces coelicolor* M-145. Appl. Biochem. Microbiol. 59 (4), 450–455. https://doi.org/10.1134/S0003683823040130.

Thiel, K., Vuorio, E., Aro, E.-M., Kallio, P.T., 2017. The effect of enhanced acetate influx on *Synechocystis* sp. PCC 6803 metabolism. Microb. Cell Factories 16 (1), 21. https://doi.org/10.1186/s12934-017-0640-x.

Weinert, B.T., Iesmantavicius, V., Wagner, S.A., Schölz, C., Gummesson, B., Beli, P., Nyström, T., Choudhary, C., 2013. Acetyl-phosphate is a critical determinant of lysine acetylation in *E. coli*. Mol. Cell 51 (2), 265–272. https://doi.org/10.1016/j.molcel.2013.06.003.

Wellburn, A.R., 1994. The spectral determination of chlorophylls *a* and *b*, as well as total carotenoids, using various solvents with spectrophotometers of different resolution. J. Plant Physiol. 144 (3), 307–313. https://doi.org/10.1016/S01761617(11)81192-2.

Wolfe, A.J., 2005. The acetate switch. Microbiol. Molecul. Biol. Rev. 69 (1), 12–50. https://doi.org/10.1128/mmbr.69.1.12-50.2005.

Xiong, W., Lee, T.-C., Rommelfanger, S., Gjersing, E., Cano, M., Maness, P.-C., Ghirardi, M., Yu, J., 2016. Phosphoketolase pathway contributes to carbon metabolism in cyanobacteria. Nat. Plants 2 (1), 15187. https://doi.org/10.1038/nplants.2015.187.

Yang, W., Catalanotti, C., D'Adamo, S., Wittkopp, T.M., Ingram-Smith, C.J., Mackinder, L., Miller, T.E., Heuberger, A.L., Peers, G., Smith, K.S., Jonikas, M.C., Grossman, A.R., Posewitz, M.C., 2014. Alternative acetate production pathways in *Chlamydomonas reinhardtii* during dark anoxia and the dominant role of chloroplasts in fermentative acetate production. Plant Cell 26 (11), 4499–4518. https://doi.org/10.1105/tpc.114.129965.

Zhou, J., Zhang, H., Zhang, Y., Li, Y., Ma, Y., 2012. Designing and creating a modularized synthetic pathway in cyanobacterium *Synechocystis* enables production of acetone from carbon dioxide. Metabol. Eng. 14 (4), 394–400. https://doi.org/10.1016/j.ymben.2012.03.005.

Zhu, J., Liu, W., Guo, L., Tan, X., Sun, W., Zhang, H., Zhang, H., Tian, W., Jiang, T., Meng, W., Liu, Y., Kang, Z., Gao, C., Lü, C., Xu, P., Ma, C., 2024. Acetate production from corn stover hydrolysate using recombinant *Escherichia coli* BL21 (DE3) with an EP-bifido pathway. Microb. Cell Fact. 23, 300. https://doi.org/10.1186/s12934-024-02575-y.